

Univolatility Curves in Ternary Mixtures: Topology and Bifurcation

Nataliya Shcherbakova^{a*}, Ivonne Rodriguez Donis^b, Jens Abildskov^c, Vincent Gerbaud^a

^aLaboratoire de Génie Chimique, Université de Toulouse, CNRS, INP, UPS, Toulouse, France

^bLaboratoire de Chimie Agro-Industrielle de Génie Chimique, INP-ENSIACET Laboratoire de Chimie Agro-Industrielle, Université de Toulouse, INRA, INP, Toulouse, France

^cPROSYS, Department of Chemical and Biochemical Engineering, Technical University of Denmark, Denmark
nshcherb@ensiacet.fr

The topological structure of univolatility curves of ternary homogeneous mixtures is derived from the boiling temperature and univolatility hypersurfaces geometry. The key point is the concept of the generalized univolatility curve in the 3D state space, which allows putting in evidence the bifurcation mechanism of the sets of the univolatility curves and to tune-up an efficient numerical algorithm for their computation by a simple integration of a system of ordinary differential equations. Two examples of different two types of bifurcation are presented by varying pressure in order to modify the topology of the ternary residue curve map.

1. Introduction

Preliminary conceptual design of distillation processes is based on the knowledge of the mixture thermodynamics and on the analysis of the residue curve maps (RCMs). The change of the volatility order between two components i and j in a ternary diagram can be detected by tracing the associated univolatility curve (or α -curve) $\alpha_{i,j}$, i.e., the set of points of equality between the distribution coefficients K_i and K_j (Kiva et al., 2003). Univolatility curves divide the composition space into different K -order regions, even for zeotropic mixtures. Their knowledge is essential to design extractive distillation process (Gerbaud and Rodriguez-Donis, 2014). Though the computation of univolatility curves starting at azeotropic points is straightforward, the detection of univolatility curves not associated with azeotropes is a more complicated and time-consuming process. A ternary diagram may contain up to 3 families of α -curves defined by their respective index. Zhvanetskii et al. (1988), Reshetov et al. (1990) and Reshetov and Kravchenko (2007, 2010) formulated the main principles of classification of the univolatility curves. They propose to distinguish the univolatility curves of type $\overline{\alpha}_{i,j}$ connecting two points on the same binary side of the composition triangle from the curves of type $\overline{\overline{\alpha}}_{i,j}$ connecting two different binary sides. Transitions between types $\overline{\alpha}_{i,j}$ and $\overline{\overline{\alpha}}_{i,j}$ can occur as univolatility curves depend on pressure and temperature of vapor – liquid equilibrium (VLE).

The new point of view on the univolatility curves proposed in this paper is based on the key role played by the temperature among the state variables of the problem. We show that the topological structure of univolatility curves follows from mutual arrangement of the boiling temperature surface and the three univolatility hypersurfaces in the 3D composition – temperature state space. By introducing the notion of a generalized univolatility curve, the computations of the univolatility curves in the inner part of the composition triangle reduces to an integration of a system of ordinary differential equations. Under variation of the pressure, the topological structure of the univolatility curves changes. The exact conditions of the bifurcation are related to the degeneracy of the generalized univolatility curve. The proposed geometrical construction is illustrated by two examples: hexafluorobenzene - methyl propionate - benzene and methyl ethyl ketone – cyclohexane – 2-methylpropanol, showing two types of possible transitions in the topology of the univolatility curves under pressure variation.

2. 3D geometry of univolatility curves

2.1 Univolatility in the temperature-concentration state space

Consider an open evaporation process of a homogeneous ternary mixture maintained under vapour liquid equilibrium (VLE) condition at constant pressure. Denote by x_i, y_i and T the mole fractions of the components in the liquid and vapour phases and the temperature. Since $x_1 + x_2 + x_3 = 1$, only two mole fractions are independent. Hence the state space of the problem has dimension 3 and can be represented as a 3D space with Cartesian coordinates (x_1, x_2, T) . The boiling temperature $T = T_b(x_1, x_2)$ of the mixture is implicitly defined by the equation

$$\Phi(x_1, x_2, T) = \sum_{i=1}^3 y_i(x_1, x_2, T) - 1 = 0 \quad (1)$$

The VLE condition can be described in terms of distribution coefficients K_i so that $y_i(x_1, x_2, T) = K_i(x_1, x_2, T) x_i$. The sets of points on the concentration plane (x_1, x_2) where $\alpha_{ij} = \frac{K_i}{K_j} = 1$ form the univolatility curves between components i and j . In the 3D complete concentration – temperature state space, Equation (1) defines the boiling temperature surface of the system, while the univolatility relations

$$\Psi_{ij}(x_1, x_2, T) = K_i(x_1, x_2, T) - K_j(x_1, x_2, T) = 0, \quad i, j = 1, 2, 3 \quad (2)$$

describe three univolatility hyper-surfaces. The intersections of these three univolatility hyper-surfaces with the boiling temperature surface give rise to the generalized univolatility curves in the concentration–temperature space, which projects onto univolatility curves on the concentration plane. Figure 1 illustrates these concepts for the case of acetone (x_1) – ethyl acetate (x_2) – benzene mixture, which has one univolatility curve $\alpha_{23} = 1$.

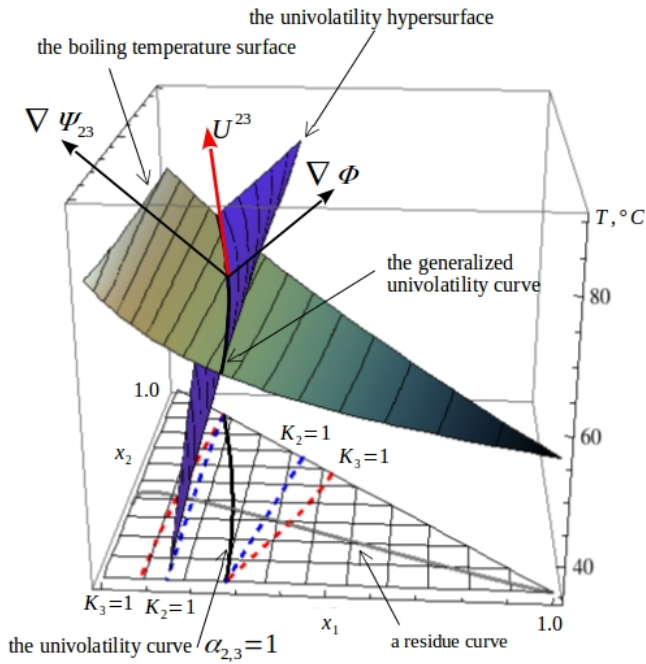


Figure 1: Mixture acetone (x_1) – ethyl acetate (x_2) – benzene: boiling temperature surface, 2-3 univolatility hyper-surface, $\alpha_{23} = 1$ univolatility curve. (adapted from Shcherbakova et al., 2017).

By construction, the generalized univolatility curve belongs both to the boiling temperature and to the univolatility hypersurfaces. So it is necessarily orthogonal to the two normal directions to these surfaces defined by the gradients of the functions Φ and Ψ_{ij} . Hence, the vector $U^{ij} = \nabla\Phi \times \nabla\Psi_{ij}$ defines the tangent direction of the generalized univolatility curve (see in Figure 1). More precisely, given an initial point, the generalized univolatility curve between the components i and j can be computed by solving the system of ordinary differential equations:

$$\dot{x}_1 = U_1^{ij}(x_1, x_2, T), \quad \dot{x}_2 = U_2^{ij}(x_1, x_2, T), \quad \dot{T} = U_3^{ij}(x_1, x_2, T) \quad (3)$$

2.2 Bifurcation of the topological structure of univolatility curves

Kiva et al. (2003) provided an exhaustive description of the properties of the univolatility curves. Each pair of the components of the mixture may have one or more univolatility curves. Therefore the related RCM may contain up to three families of univolatility curves of different index ij . Each binary azeotrope gives rise to an univolatility curve, while the intersection point of three of such curves of different families corresponds to a ternary azeotrope. In addition, there exist univolatility curves not connected to azeotropes. All these properties are the base of the topological classification of the univolatility curves proposed in Zhvanetskii et al (1988), Reshetov et al. (1990) and Reshetov and Kravchenko (2010). The curves of type $\overline{\alpha}_{i,j}$ connect two points on the same binary side of the composition triangle, while the $\overline{\overline{\alpha}}_{i,j}$ type curves connect two opposite binary sides. The transition between two types may occur under the modification of the process conditions.

In the case of isobaric distillation, variation of the pressure causes the transformation of the shape of the boiling temperature surface, and consequently the shape of the univolatility curves. At the critical value of the pressure, the boiling temperature surface and one of the univolatility hyper-surfaces have a common tangent point, in other words, the vector U^{ij} is zero. An accurate computation shows that

$$U_3^{ij} = U_1^{ij} \frac{\partial T_b}{\partial x_1} + U_2^{ij} \frac{\partial T_b}{\partial x_2} \quad (4)$$

This means that there is a one to one correspondence between the singular points of the generalized univolatility curve and its projection on the concentration triangle. Therefore the exact bifurcation conditions for the curve $\alpha_{ij} = 1$ can be found by solving the following system of equations with respect to x_1^* , x_2^* , T^* and P^* :

$$\Phi(x_1^*, x_2^*, T^*, P^*) = 0, \quad \Psi_{i,j}(x_1^*, x_2^*, T^*, P^*) = 0, \quad U_1^{ij}(x_1^*, x_2^*, T^*, P^*) = 0, \quad U_2^{ij}(x_1^*, x_2^*, T^*, P^*) = 0 \quad (5)$$

At $P = P^*$ the α –curve under consideration has a singular point at the point x_1^*, x_2^* on the concentration triangle. In principle, such a point can be of elliptic or hyperbolic type. The latter describes the transition between $\overline{\alpha}_{i,j}$ and $\overline{\overline{\alpha}}_{i,j}$ types, the corresponding univolatility curve is formed of two branches meeting at the singular point.

It is worth to underline that in general the singular points of the univolatility curves are not related to azeotropes, though in some exceptional cases they can coincide with singular azeotropes or pure states, as it is illustrated in Section 3.2. This fact makes the numerical computation of the univolatility curves much simpler than the computation of the residue curves.

2.3 From geometry to numerical computation

The system of Equations (3) can be used for the efficient numerical computation of the univolatility curves by using the standard Runge-Kutta schemes. The details of this method can be found in Shcherbakova et al. (2017). The integration starts at the points on the binary sides of the concentration triangle satisfying the univolatility condition. They can be found by analysing the behaviour of the binary distribution coefficients K_i , as proposed in Kiva et al. (2003).

For example, in order to compute a curve $\alpha_{ij} = 1$ starting from the 13 binary side, one need first to find a point $(x_{1,ij}^0, 0, T_{1,ij}^0)$ in temperature - concentration state space. Then the rest of the curve can be computed by solving the following initial value problem:

$$\frac{dx_1}{ds} = \frac{d_{ij} U_1^{ij}(x_1, x_2, T)}{\|U^{ij}(x_1, x_2, T)\|}, \quad \frac{dx_2}{ds} = \frac{d_{ij} U_2^{ij}(x_1, x_2, T)}{\|U^{ij}(x_1, x_2, T)\|}, \quad \frac{dT}{ds} = \frac{d_{ij} U_3^{ij}(x_1, x_2, T)}{\|U^{ij}(x_1, x_2, T)\|} \quad (6)$$

$$x_1(0) = x_{1,ij}^0, \quad x_2(0) = 0, \quad T(0) = T_{1,ij}^0, \quad d_{ij} = \text{sign}(U_2^{ij}(x_{1,ij}^0, 0, T_{1,ij}^0)) \quad (7)$$

Here s is the arc-length of the curve. The normalized form of Equation (6) avoid the eventual stiffness problem, while the coefficient $d_{ij} = \pm 1$ indicates the direction pointing inside the composition triangle. In the next Section, the results of the application of the prototype of this algorithm realized in Mathematica 9 are presented.

3. Case studies

The efficiency of the algorithm described above is illustrated by detecting the bifurcations conditions for two ternary mixtures. Residue curve map of hexafluorobenzene - methyl propionate - benzene has the particularity of having two binary azeotropes for the mixture hexafluorobenzene - benzene. The second example, methyl ethyl ketone - cyclohexane – 2-methylpropanol, exhibits the bifurcation of the univolatility curve through the formation of the singular pure state.

3.1 Hexafluorobenzene-methyl propionate-benzene

Figure 2 illustrates the bifurcation of the topological structure of α -curves of the ternary mixture hexafluorobenzene (x_1) – methyl propionate (x_2) – benzene (the origin) through the formation of the hyperbolic singular point described in Section 2.2.

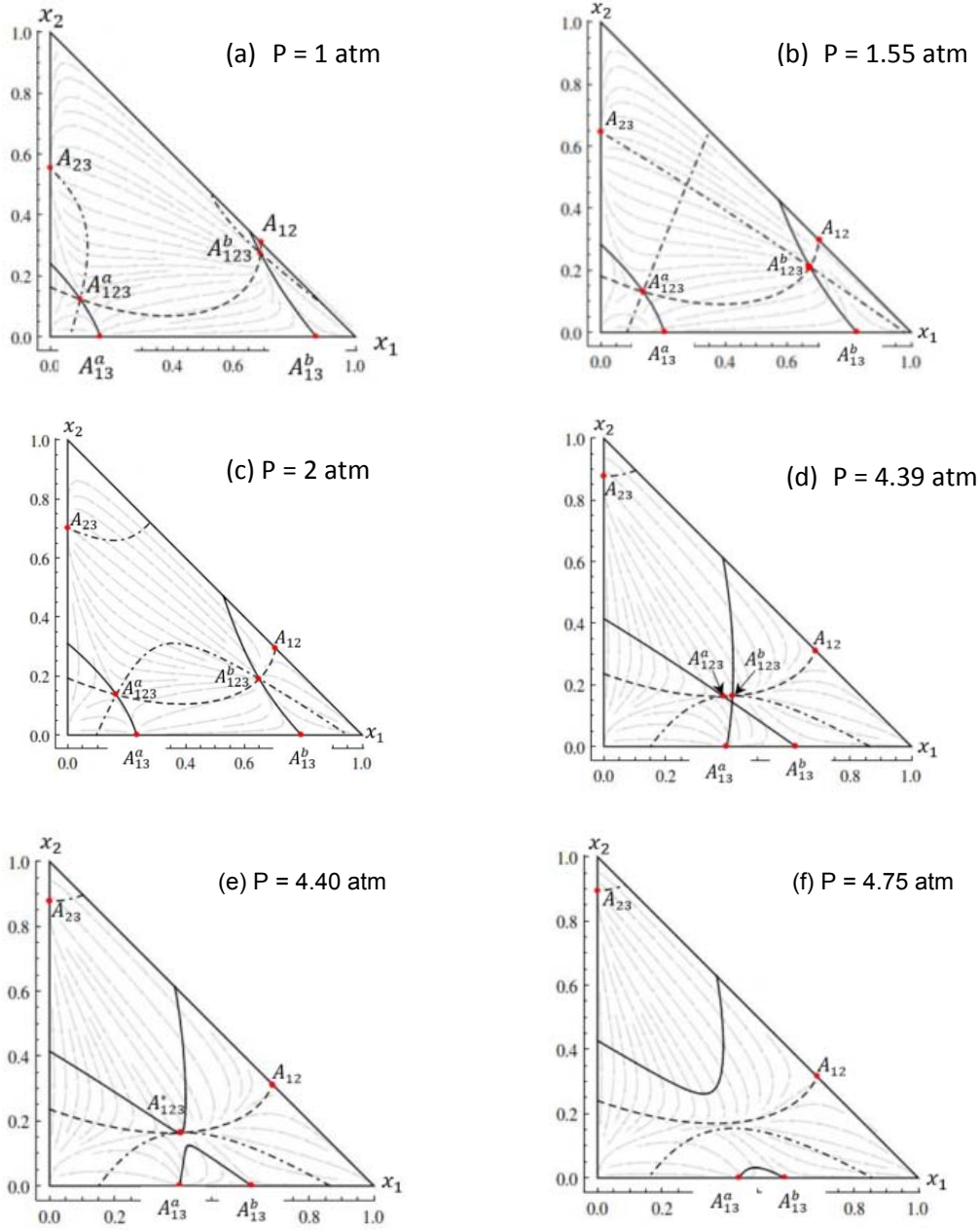


Figure 2: Hexafluorobenzene (x_1) - methyl propionate (x_2) - benzene (the origin), RCM and univolatility curves: $\alpha_{12} = 1$ (dashed line), $\alpha_{13} = 1$ (continuous line), $\alpha_{23} = 1$ (dot dashed line) at different pressures.

The computations in Figure 2 were done applying the algorithm described in Section 2. The VLE parameters (see in Table 1) were computed according to Wilson's model using the data from Myagkova (2007). The vapor pressure was computed by using the models and their constants available in DIPPR database.

At 1 atm (Figure 2a) the binary mixture benzene - hexafluorobenzene exhibits two azeotropes A_{13}^a, A_{13}^b . Each of these gives rise to a univolatility curve of $\overline{\alpha}_{1,3}$ type. The binary azeotrope A_{23} (benzene-methyl propionate) is the origin of a $\overline{\alpha}_{2,3}$ curve. The other curve of the same index, of $\overline{\alpha}_{2,3}$ type, links two non-azeotropic points on the 12-side. The binary azeotrope A_{12} (hexafluorobenzene – methyl propionate) gives rise to the unique $\overline{\alpha}_{1,2}$ type curve. Such a complex structure of α -curves reflects a peculiar topology of the underlying RCM

characterized by two ternary azeotropes: a saddle (A_{123}^a) and a stable node (A_{123}^b). Under higher values of the pressure, the two curves $\bar{\alpha}_{2,3}$ get closer, and at $P \approx 1.55$ atm (Figure. 2b) the first bifurcation occurs: the two curves $\bar{\alpha}_{2,3}$ form a singular cross-shape configuration described in Section 2.2. With the infinitesimal pressure increase, this singular configuration splits into a $\bar{\alpha}_{2,3}$ curve connected to A_{23} and a new $\bar{\alpha}_{2,3}$ curve linking two non-azeotropic points on the 13-side (Figure 2c). Meanwhile the two branches of the $\alpha_{1,3}$ curve get closer as well as two ternary azeotropes. At $P \approx 4.39$ atm (Figure 2d) the second bifurcation occurs in the $\alpha_{1,3}$ curve. The singular configuration splits into a $\bar{\alpha}_{1,3}$ and $\bar{\alpha}_{1,3}$ branches with the further pressure increase and at $P \approx 4.40$ atm (Figure 2e) the two ternary azeotropes merge into a unique singular azeotrope A_{123}^* of saddle-node type, which disappears at higher values of pressure (Figure 2f).

Table 1: Example 1, Wilson's model binary interaction parameters (Myagkova, 2007), Cal/mom

component i	component j	λ_{ij}	λ_{ji}
hexafluorobenzene	methyl propionate	7.854	-35.152
hexafluorobenzene	Benzene	1218.177	-445.561
methyl propionate	Benzene	98.176	7.033

3.2 Methyl ethyl ketone – cyclohexane – 2-methyl propanol

The next example shows the transition between $\bar{\alpha}_{i,j}$ and $\bar{\alpha}_{i,j}$ types with formation of the singularity at one of the pure states of the system in the mixture methyl ethyl ketone – cyclohexane - 2-methyl propanol. The computations were done using the NRTL model for the binary coefficients (Table 2). The vapor pressure was computed by using the models and their constants available in DIPPR database.

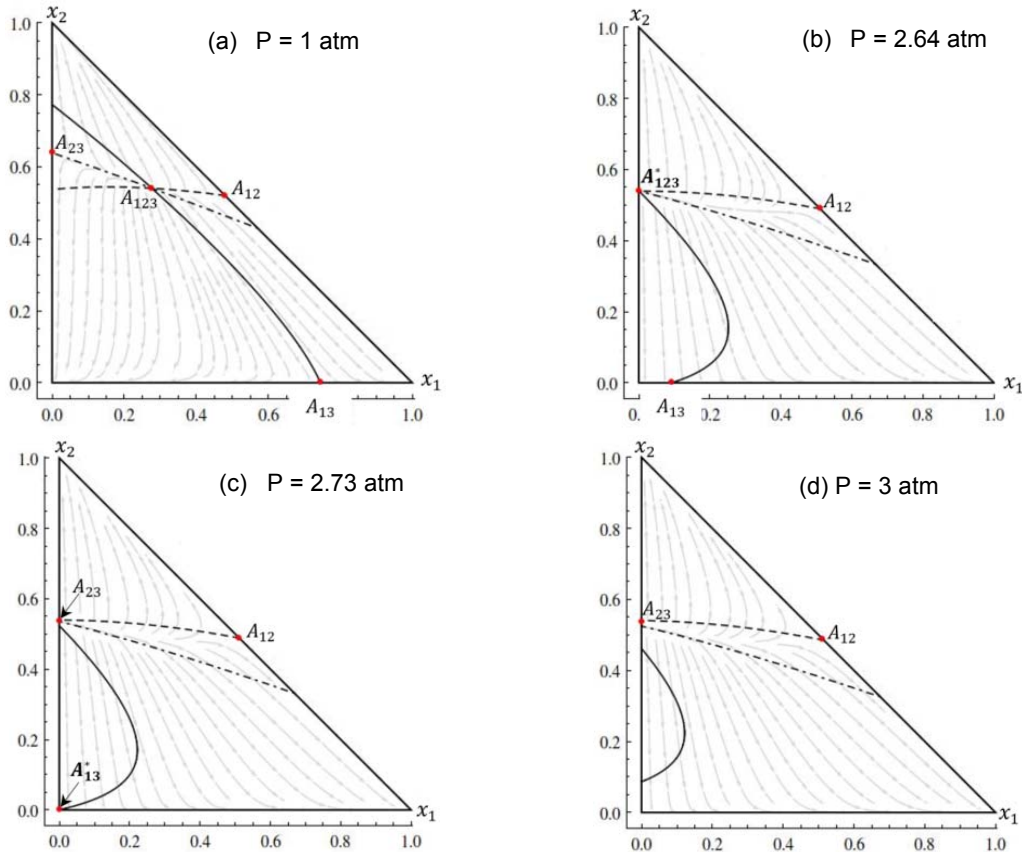


Figure 3: Methyl ethyl ketone (x_1) - cyclohexane (x_2) – 2-methyl propanol (the origin), RCM and univolatility curves: $\alpha_{12} = 1$ (dashed line), $\alpha_{13} = 1$ (continuous line), $\alpha_{23} = 1$ (dot dashed line) at different pressures

Table 2: Example 2, NRTL model binary interaction parameters $a_{ij} = a_{ij}^0 + a_{ij}^1 T$, Cal/mol

component <i>i</i>	component <i>j</i>	a_{ij}^0	a_{ij}^1	a_{ji}^0	a_{ji}^1	α_{ij}
methyl ethyl keton	cyclohexane	97.3520	0	750.176	0	0.3
methyl ethyl keton	2-methyl propanol	-62.315	6.0050	512.095	-7.741	0.3
cyclohexane	2-methyl propanol	1067.39	2.125	366.122	-2.73	0.47

At 1 atm (Figure 3a) the RCM of this mixture is characterized by three binary azeotropes of saddle type on each binary side of the composition triangle. Three univolatility curves $\overline{\alpha}_{1,2}$, $\overline{\alpha}_{1,3}$ and $\overline{\alpha}_{2,3}$ start from binary azeotropes and intersect at the ternary azeotrope A_{123} (unstable node). The increment of the pressure to 2.64 atm causes the fusion of the ternary azeotrope with binary azeotrope A_{23} of saddle type and the resulting binary azeotrope A_{123}^* is a singular point (Figure 3b). At slightly higher values of the pressure this singular azeotrope splits into two, but only one of them, the binary azeotrope A_{23} of unstable node type remains on the binary side of the composition triangle. At the same time the binary azeotrope A_{13} , which belongs to the $\overline{\alpha}_{1,3}$ curve, moves to the left towards the apex of the pure 2-methyl propanol. With the further pressure increment, at $P \approx 2.73$ atm, this azeotrope merges with the pure 2-methyl propanol state (the point A_{13}^* in Figure 3c) forming a tangential singularity. Physically this means that within the NRTL model, the first two components, cyclohexane and 2 methylpropanol, have equal volatilities at infinite dilution at 2.73 atm. The described singularity is destroyed by the infinitesimal increasing of the pressure, and the bottom end point of the $\alpha_{1,3} = 1$ curve moves to the 2-3 (cyclohexane – 2-methyl propanol) binary side. The resulting univolatility curve $\overline{\alpha}_{1,3}$ connects two non-azeotrope compositions on the 2-3 side.

4. Conclusions

The topological structure of RCMs and associated univolatility curves is non-trivial even in the case of zeotropic ternary mixtures (Reshetov and Kravchenko, 2007). The standard 2D representation in the composition space is not always sufficient to describe the true nature of the univolatility curves. A more rigorous 3D description based on the concept of the generalized univolatility curve puts in evidence the mechanism of formation of α -curves in the ternary composition space and their transformation under the variation of the process conditions. The computational efficiency of the resulting numerical algorithm is illustrated by tracing the bifurcation in the univolatility curves topology with pressure variation in two ternary azeotropic mixtures, hexafluorobenzene – methyl propionate – benzene and methyl ethyl ketone – cyclohexane – 2-methylpropanol. The proposed method allows computing detailed phenomena like the formation of tangential azeotrope, bi-ternary azeotropy, saddle-node azeotropes as well as to detect the exact bifurcation conditions in the global structure of the univolatility curves of ternary mixtures.

References

- Gerbaud V., Rodriguez-Donis I., 2014, Extractive distillation. chap. 6. "Distillation Book", Vol. II Distillation: equipment and processes. Ed. Gorak, A., Olujić, Z. Elsevier, Amsterdam, 201–246.
- Kiva V.N, Hilmen E.K., Skogestad S., 2003, Azeotropic phase equilibrium diagrams: a survey. Chemical Engineering Science, vol. 58, 1903–1953.
- Myagkova T.O., 2007. Physicochemical foundations of separation of bazeotropic mixtures. Extract of PhD Thesis, Moscow. (dlib.rsl.ru/01003175223)
- Prosim S.A, 2017, Simulis Thermodynamics Manual, <http://www.prosim.net/en/software-simulis-thermodynamics-mixture-properties-and-fluid-phase-equilibria-calculations-3.php>
- Reshetov S.A., Sluchenkov V.Yu, Ryzhova V.S., Zhvanetskii I.B., 1990, Diagrams of K-Ordered Regions with An Arbitrary Number of Unitary α -lines, Russian Journal of Physical Chemistry, 64(9), 1344–1347.
- Reshetov S.A., Kravchenko S.V., 2007, Statistics of liquid-vapor phase equilibrium diagrams for various ternary zeotropic mixtures. Theoretical Foundations of Chemical Engineering, 41(4), 439–441.
- Reshetov S.A., Kravchenko S.V., 2010, Statistical analysis of the kinds of vapor-liquid equilibrium diagrams of +three-component systems with binary and ternary azeotropes, Theoretical Foundations of Chemical Engineering, 44(3), 279–292.
- Shcherbakova N., Rodriguez-Donis I., Abildskov J, Gerbaud V. 2017. A novel method for detecting and computing univolatility curves in ternary mixtures, Chemical Engineering Science, 173, 21–36.
- Zhvanetskii I.B., Reshetov S.A., Sluchenkov V.Yu., 1988, Classification of K-order regions on the distillation line diagram for a ternary zeotropic system, Russian Journal of Physical Chem, 62(7), 996–998.